PROCEEDINGS of the
23rd International Congress on Acoustics

9 to 13 September 2019 in Aachen, Germany

Analysis of displacement amplification characteristics of class IV flextensional shell based on elliptic perimeter approximation formula

Houlin FANG[1]; Difeng SUN; Fang ZHANG; Yang LIU; Tianqing ZHAO; Zhang CHENG; Liangyong ZHANG; Xubin LIANG; Deyu SUN

[1] Northwest Institute of Nuclear Technology, China

ABSTRACT

As the most widely used underwater acoustic transducer, class IV flextensional transducer can get larger amplitude flexural vibration from longitudinal vibration of driven stack by the displacement amplification effect, thereby radiating more energy. In order to further quantitatively understand the displacement amplification characteristics of elliptical tube shell, this paper proposed to calculate the displacement magnification using the ellipse perimeter approximation formula, and the variation law of the displacement amplification with the compression coefficient and the deformation rate was obtained, which was analysed and compared with the results by the method of finite element analysis. The empirical formula for calculating the finite element results by the results of the perimeter approximation formula was got by fitting curves. When the compression coefficient is 0.24~0.80, the error of the calculation results was not more than 6.11%. The research of this paper has certain reference significance for the estimation of the radiation performance of low frequency transducers.

Keywords: Displacement magnification, Class IV flextensional shell, Elliptic perimeter approximation formula

1. INTRODUCTION

Underwater acoustic transducers which plays an important role on sound information translation are widely used in ocean monitoring, underwater communication, marine resources development and so on(1). As a member of underwater acoustic transducers, class IV flextensional transducer can get larger amplitude flexural vibration from longitudinal vibration of driven stack by the displacement amplification effect, thereby radiating more energy. Due to advantages such as low frequency, high power and small size, class IV flextensional transducer has always been a research hotspot, so that is the most widely studied and analyzed.

The research of class IV flextensional transducers is mainly reflected in the two aspects of materials and structures. The materials are mainly driven materials research, supplemented by shell materials research. The traditional driven material is piezoelectric ceramics. In recent years, rare earth giant magnetostrictive materials(Terfenol-D) have been applied to a large extent, and some newly developed materials such as antiferroelectric ceramics and single crystal materials are also applied in class IV flextensional transducers. Transducer structure is rich in research. In recent years, transducers with low frequency, wideband and high power have been the main research directions. Fish-lip flextensional transducer invented by Mo Xiping have adopted a variable-height elliptical shell, which makes the shell have both a double-amplification effect (2).The frequency can be effectively widened by slitting the radiating surface of the shell. The Institute of Acoustics of the Chinese Academy of Sciences and the Harbin Engineering University have in-depth research (3-5).

In order to maximize the radiated sound power while ensuring the broadband performance of the transducer, Lan Yu and Mo Xiping have developed a double-shell flextensional transducer (6), which maximizes the volume displacement output of the transducer to achieve low frequency and high power acoustic radiation. In 2011, Indian scholars (7) proposed a flextensional transducer with a parabolic reflector with a gain of 1.7-8dB. Multi-mode coupling through the shell is also an effective means of

[1] fanghoulin@nint.ac.cn

expanding the frequency band and many scholars have done a lot of work (8, 9).In 2017, Wang Yue studied waterdrop type flextensional transducer based on antiferroelectric ceramics, which effectively expanded the bandwidth by first asymmetric bending mode and first bending mode coupling(10). Zhou Tianfang(11) proposed a transducer structure that is conformally driven with shell, which can effectively avoid the change of vibration mode caused by the traditional longitudinal drive crystal stack, and can obtain a lower frequency.

In terms of driving materials, the erbium-doped antiferroelectric ceramics(PLZST) of the Xi'an Jiaotong University was first applied in class IV flextensional transducer(12).Li Kuan *et al*. studied a Class IV rare-earth flextensional transducer(13).

Although research on class IV flextensional transducer is so adequate there are few studies on the displacement amplification characteristics. In the literatures(14,15) only the displacement amplification schematic diagram is given, and the displacement amplification effect is briefly described. However, there are few quantitative studies on the displacement amplification characteristics of the flextensional shell, especially the displacement magnification. Therefore, for the need of for class IV flextensional transducer in air, this paper proposed a method to estimate the displacement magnification using the approximate perimeter formula, and the variation law of the displacement magnification with the compression coefficient and deformation rate was obtained, which was analyzed and compared with FEA results. The work of this paper has certain reference significance for the estimation of radiation performance of low frequency transducers.

2. THEORETICAL CALCULATION

2.1 Derivation of Displacement Magnification

The shell of class IV flextensional transducer is an elliptic cylindrical shell, which is simplified to a neutral plane ellipse with long-axis $2a$, short-axis $2b$ ($a>b$) , focal length $2c$ ($c=\sqrt{a^2-b^2}$) and eccentricity e ($e=c/a<1$) for convenience. When the load (force or displacement) of stack acts on the ellipse, the long-axis deformation is Δa, and the short-axis deformation is Δb (Figure 1).

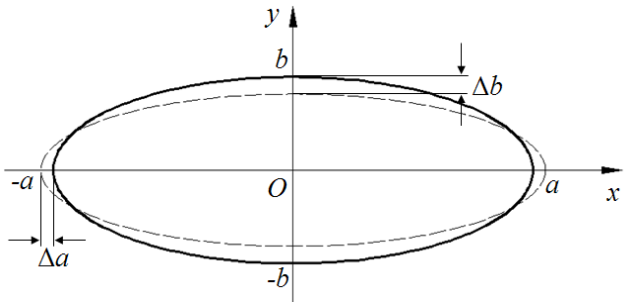

Figure 1 –Schematic diagram of neutral plane ellipse deformation

Two assumptions are made before and after ellipse deformation:(1) After deformation, especially when the deformation is relatively small, the structure is still approximate ellipse.(2) Before and after deformation, the deformation of elliptic perimeter is much smaller than that of long- and short-axis, and the elliptic perimeter is approximately unchanged. So the following derivation is made. Elliptic perimeter approximation formula is

$$L \approx \pi\left[1.5(a+b)-\sqrt{ab}\right] \tag{1}$$

Thus, elliptic perimeter of before deformation is equal to that of after deformation as following function.

$$1.5(a+b)-\sqrt{ab}=1.5(a+\Delta a+b-\Delta b)-\sqrt{(a+\Delta a)(b-\Delta b)} \tag{2}$$

Let $\Delta b/\Delta a=\alpha$, defined as displacement magnification, and is substituted into above formula to get the quadratic equation for α.

$$2.25\alpha^2+\left(\frac{a-3\sqrt{ab}}{\Delta a}-3.5\right)\alpha+\frac{3\sqrt{ab}-b}{\Delta a}+2.25=0 \tag{3}$$

The solutions is

$$\alpha = \frac{3.5 - \frac{a-3\sqrt{ab}}{\Delta a} \pm \sqrt{\left(\frac{a-3\sqrt{ab}}{\Delta a} - 3.5\right)^2 - 4 \times 2.25 \times \left(\frac{3\sqrt{ab}-b}{\Delta a} + 2.25\right)}}{4.5} \tag{4}$$

It can be seen that displacement magnification α is related to half-long-axis a, half-short-axis b and long-axis deformation Δa. Let $b/a=B$, defined as compression coefficient in mathematics. Let $\Delta a/a=A$, defined as deformation rate. So the displacement magnification expression can be simplified to(considering the actual situation, the symbol "±" should be taken as "-")

$$\alpha = \frac{3.5 - \frac{1-3\sqrt{B}}{A} - \sqrt{\left(\frac{1-3\sqrt{B}}{A} - 3.5\right)^2 - 9\left(\frac{3\sqrt{B}-B}{A} + 2.25\right)}}{4.5} \tag{5}$$

where A and B meet the following inequality group

$$\begin{cases} 0 < A < 1; \\ 0 < B < 1; \\ A > \dfrac{1-3\sqrt{B}}{3.5}; \\ 8A^2 + \left(7 + 6\sqrt{B} - 9B\right)A - \left(1 - 3\sqrt{B}\right)^2 \le 0. \end{cases} \tag{6}$$

2.2 Law of Change

Based on the above formula (5), a group of curves (Figure 2 and Figure 3) showing the relationship between displacement magnification and compression coefficient b/a and deformation rate $\Delta a/a$ is obtained. In Figure 2, as the compression coefficient increasing the displacement magnification decreases and the decrease rate gradually decreases. When compression coefficient is same, the larger deformation rate, the larger the displacement magnification. And the difference of curves decreases with the increase of compression coefficient. The minimum compression coefficient that can be solved by perimeter approximation formula is related to the deformation rate. The larger the deformation rate, the larger the minimum compression coefficient. Figure 3 gives a series of similar results, but the trend of curves is opposite. It can be known that if the perimeter approximation formula is solved, compression coefficient should not be too small and deformation rate should not be too large. Compression coefficient has a greater influence on the displacement magnification than deformation rate.

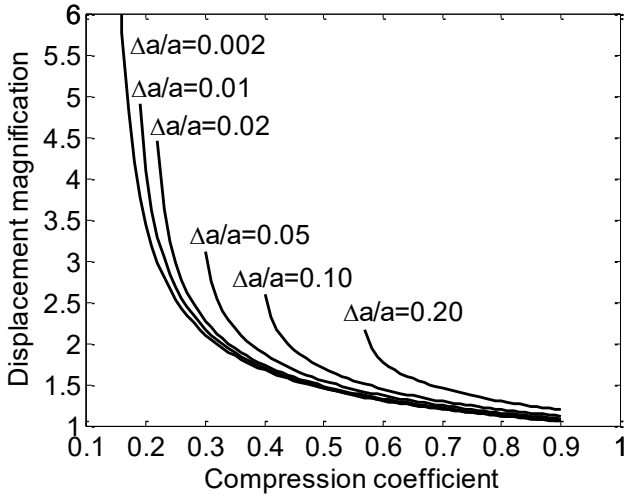

Figure 2 – Displacement magnification versus compression coefficient with different deformation rates

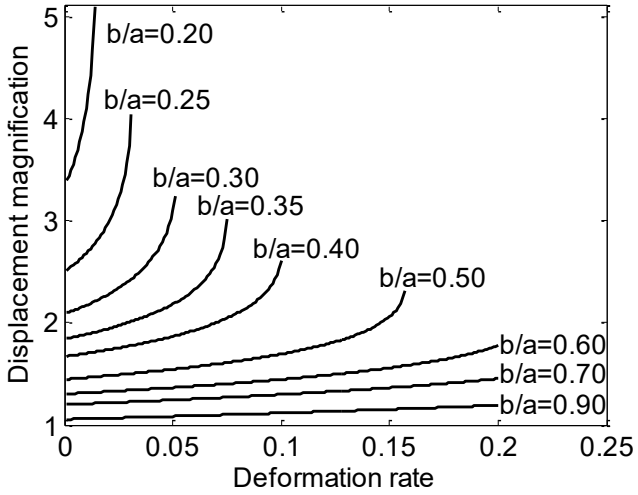

Figure 3 –Displacement magnification versus deformation rate with different compression coefficients

3. FINITE ELEMENT ANALYSIS

3.1 Modeling

The structural parameters of the class IV flextensional shell mainly include long-axis(2*a*), short-axis(2*b*), wall-thickness(*t*) and width(*B*). Combined with the analysis above, the displacement magnification is mainly related to the long-axis and the short-axis. Therefore, the long-axis and the short-axis are mainly changed, and the wall-thickness and width are only selected a value appropriately.

The FEA modeling firstly establishes the calculation model according to the parameters, then divides the grid according to the calculation requirements, sets the model load, and finally calculates the structural deformation nephogram. Further, the displacement value can be extracted to obtain the displacement magnification.

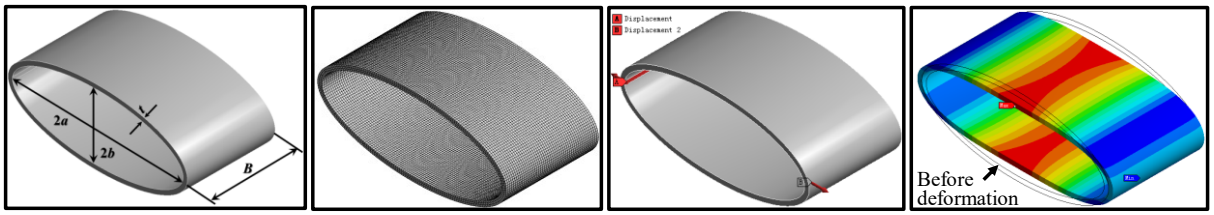

(*a*) Parameterized model (*b*) Meshing (*c*) Load setting (*d*) Deformation result

Figure 4 –FEA modeling

3.2 Law of Change

On the basis of theoretical calculation, a set of shells with different structural parameters are correspondingly designed for FEA. Figure 5 shows the displacement magnification versus compression coefficient comparing between theoretical calculation and FEA. Note that power exponent lines fit these data quite well, FEA results are higher at all compression coefficients. The difference decreases as compression coefficient increasing, when the value tends to 1, namely ellipse tends to circle, the difference tends to be zero. When the compression coefficient reaches 0.122, there is no solution by using the perimeter approximation formula, but the FEA results are still consistent with the overall law.

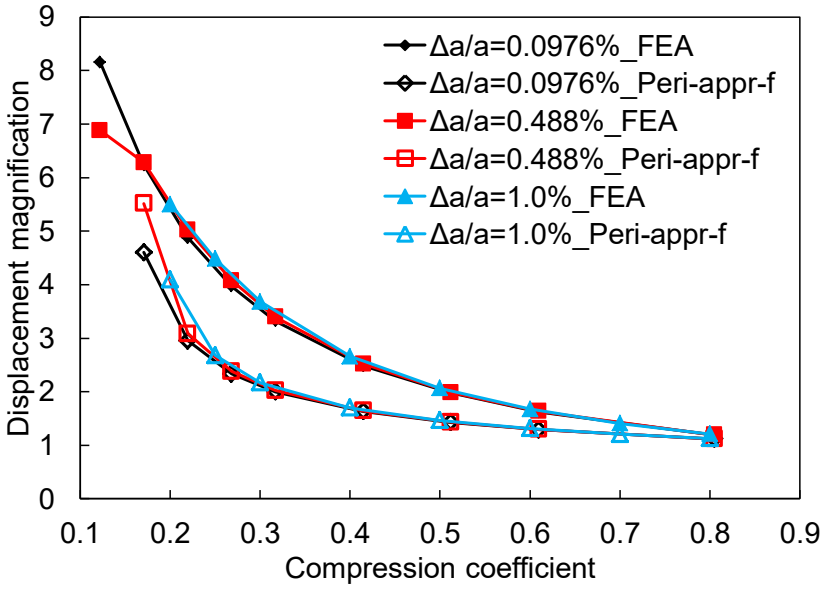

Figure 5 –Perimeter approximation formula and FEA results of displacement magnification versus compression coefficient with deformation rate is 0.0976%, 0.488% and 1.0%(which are written as % conveniently). Perimeter approximation formula is replaced by "Peri-appr-f" in the figure.

In figure 6, the curve with a compression coefficient of 0.3 is basically larger than the curve with a compression coefficient of 0.4. FEA results are generally larger than the perimeter approximation formula results with different trends. Especially, the curve with a compression coefficient of 0.3, the results of the perimeter approximation formula increases faster with the increase of deformation rate until no solution. However, the curve of FEA increases with the deformation rate, of which the rate is gradually slowed, and then the displacement magnification reaches the maximum and then begins to fall. The curve maximum point with a compression coefficient of 0.3 is smaller than the curve with a compression coefficient of 0.4.

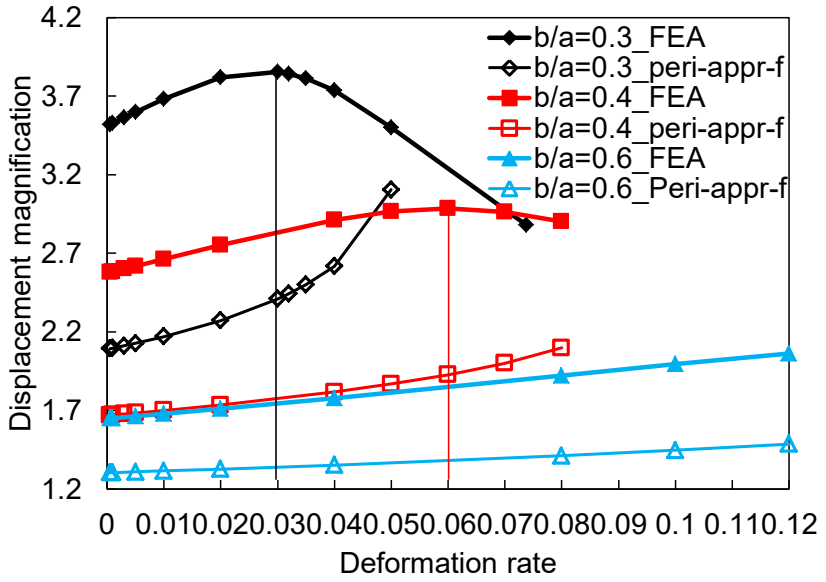

Figure 6 –Perimeter approximation formula and FEA results of displacement magnification versus deformation rate with compression coefficient is 0.3, 0.4 and 0.6. Perimeter approximation formula is replaced by "Peri-appr-f" in the figure.

In summary, the results indicates that the compression coefficient has a relatively great influence on the displacement magnification. With the chosen range of compression coefficient and

deformation rate, the maximum variation of the perimeter approximation formula results with the deformation rate is 48.4%, and the FEA results is up to 33.8%. However, the corresponding maximum variation with the compression coefficient is 392.9% and 587.1%.

4. COMPARATIVE ANALYSIS

4.1 Difference Analysis between Perimeter Approximation Formula and FEA

The displacement nephogram of FEA showing in figure 7 compares the change of the elliptical shell on which a force loaded. For convenience of analysis, draw the long- and short-axes before and after the deformation and the corresponding ellipse.

It can be seen that when the deformation displacement is large enough (for example Δa=5mm), the neutral surface of the structure is obviously no longer elliptical, the deformation in the long-axis direction is Δa, and the displacement in the short-axis direction is Δb. If the ellipse is still considered after the deformation, as shown by the black dot-dash line, the perimeter will inevitably decrease. If the perimeter is to be kept constant, the deformed ellipse should be as shown by the pink dash line ellipse. The displacement deformation in the short-axis direction is $\Delta b'$ which is smaller than Δb, so the displacement magnification obtained by theoretical calculation is smaller than the displacement magnification calculated by FEA, and the larger the displacement deformation in the long-axis direction, the larger the difference between the deformed structure and the ellipse, which will lead to the larger the difference of displacement magnification between theoretical calculation and FEA. This is the same conclusion as the previous analysis.

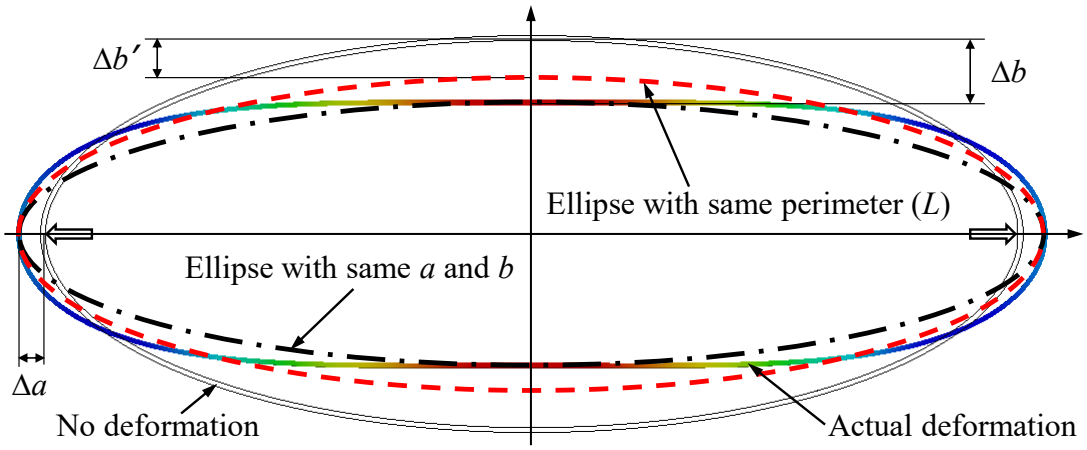

Figure 7 –Schematic diagram of before and after deformation with corresponding ellipses

4.2 FEA Curve of Deformation Rate Analysis

For the phenomenon in FEA that the displacement magnification reaches the maximum value and then falls is further analyzed. It can be seen from the lateral deformation nephogram of the shell that before the displacement magnification reaching the maximum value, the curvature direction of the short-axis end point remains unchanged after deformation (Namely the structure at the end of the short-axis is convex), but the curvature direction becomes changed (That is, the structure at the end of the short-axis becomes inwardly concave), which conforms to the actual deformation characteristics, and the structural stress also reaches the strength limit of the material. By analyzing the structures with compression coefficients of 0.3 and 0.4, the relative deformation rate of the short-axis direction when the displacement magnification reaches the maximum value is 39%-45%.

4.3 Fitting Curve Analysis

In the calculations above, in order to observe the overall trend and law of variation the range of chosen compression coefficient and deformation rate is large, and the difference between perimeter approximation formula results and FEA results is large, especially law of change with deformation rate. Considering the actual situation, the compression coefficient and deformation rate should be limited as follow:

(1) Strain of driven materials. The strain of driven materials such as piezoelectric ceramics,

rare-earth materials and antiferroelectric materials directly determines the deformation rate of shell in the long-axis direction. The strain of this kind of material is generally a few thousandths (the maximum strain of Terfenol-D is 1.5‰(1)), and the maximum strain of relaxor ferroelectric single crystal is up to 1.7%, so the maximum deformation rate is recommended as 2% (0.02).

(2) Using the approximation formula for calculation, the difference will increase when there is no solution. At the same time, the compression coefficient will be generally less than 0.2 with which the shell is extremely narrow this structure and is rarely used. Therefore, the recommended compression coefficient is chosen to be a minimum of 0.2.

Based on two points above, fitting curves of displacement magnification versus compression coefficient gets the relation of displacement magnification between perimeter approximation formula and FEA:

$$\alpha_{\text{FEA}} = 1.053\left(\frac{b}{a}\right)^{-0.355} \alpha_{\text{peri-appr-f}} \tag{7}$$

A set of flextensional shells are designed, first estimated by empirical formula (7), and then calculated by FEA to verify the accuracy of the estimation. Table 1 lists the calculation results, which shows that the empirical formula can be used to calculate the FEA results from the results of the perimeter approximation formula, and the calculation error is not more than 6.11% when the compression coefficient is 0.24~0.80.

Table 1 –Results of estimation by empirical formula

NO.	b/a	a/mm	b/mm	$\Delta a/a$	Δa/mm	Perimeter Appro-f	Estimation of FEA	FEA	Error
1	0.20	100	20	0.01	1	4.090	7.626	5.500	38.65%
2	0.22	100	22	0.01	1	3.285	5.921	5.089	16.35%
3	0.24	100	24	0.01	1	2.841	4.965	4.679	6.11%
4	0.25	100	25	0.01	1	2.681	4.618	4.486	2.94%
5	0.60	100	60	0.02	2	1.326	1.674	1.709	2.05%
6	0.80	100	80	0.02	2	1.133	1.290	1.226	5.22%

5. PRELIMINARY CONCLUSIONS

According to the calculation of the perimeter approximation formula and FEA results, the influence of the compression coefficient on the displacement magnification is greater than the deformation rate. FEA results are larger than the results of perimeter approximation formula.

With the increase of compression coefficient the displacement magnification decreases as power exponential. The same compression coefficient, the larger the deformation rate, the larger the displacement magnification, but the difference is not obvious. With the increase of compression coefficient, the difference between the FEA results and perimeter approximation formula results decreases.

Law of change with deformation rate, the difference between the FEA results and perimeter approximation formula results is large, especially with smaller compression coefficient. Firstly the displacement magnification increases with the deformation rate, the growth rate is gradually slowed, and then began to fall after reaching the maximum value. The curve maximum point with a compression coefficient of 0.3 is smaller than the curve with a compression coefficient of 0.4.

When the compression coefficient is 0.24~0.80 and the deformation rate is less than 2%, the empirical formula can be used to calculate the FEA results from the results of the perimeter approximation formula, and the calculation error is not more than 6.11%.

ACKNOWLEDGEMENTS

The authors would like to thank the Acoustic Engineering Innovation Group Fund for funding this project, and also would like to thank every member of the project team for their contribution to the work of this paper. This work would not have been possible without your help.

REFERENCES

1. Yang RY. Research on Major Axis Lengthened Rare Earth Flextensional Transducer. Harbin Engineering University;2016.
2. Mo XP. Development of underwater acoustic transducers. Applied Acoustics.2012;31(3):171-177.
3. Mo XP, Zhu HQ. A New Design of Low-frequency Broadband Flextensional Transducer. Proceedings of 2nd International Conference & Exhibition on Underwater Acoustics Measurements; June 2007;Greece, 2007.p.1391.
4. Lan Y. Research on low frequency broadband flextensional transducer. Harbin Engineering University;2005.
5. Chen S, Lan Y. Finite element analysis of flextensional transducer with slotted shell. Applied Mechanics and Materials, 2013;187:151-154.
6. Chen Z. The Research of Double-shell Flextensional Transducer. Harbin Engineering University;2016.
7. Moosad KPB, Chandrashekar G, Joseph MJ, John R. Class IV Flextensional Transducer with a reflecto. Applied Acoustics. 2011;(72):127-131.
8. Li ZQ, Mo XP, Zhang YQ, et al. Design of grooved outboard-driven class IV flextensional transducer. Technical Acoustics. 2015; 34(6): 566-569.
9. Li ZQ, Mo XP, Zhang YQ, et al. Dual elliptical shells serially connected broadband flextensional transducer. Acta Acustica. 2016; 41(4) : 494-498.
10. Wang Y. Research on Anti-ferroelectric Ceramics Flextensional Transducer. Harbin Engineering University;2017.
11. Zhou TF, Lan Y, Zhang QC, et al. A Conformal Driving Class IV Flextensional Transducer. Sensors. 2018;18: 2102.
12. Lv KJ, Li JB, Xing JX, Yin YL. Antiferroelectric phase transitions ceramics low frequency projector. Acta Acustica. 2011; 36(5):520-526.
13. Li K, Lan Y. Research of a Class IV rare-earth flextensional transducer. Technical Acoustics. 2015; 34(5):467-471.
14. Shi WD. The Research of Multi-Displacement Amplify Low Frequency Flextensional Transducer. Harbin Engineering University;2012.
15. Lan Y, Wang ZY, Wang WZ. Design of flextensional transducer based on finite element method. Technical Acoustics. 2005; 24(4):268-271.